Science Advances
AAAS

advances.sciencemag.org/cgi/content/full/4/11/eaau4637/DC1

# Supplementary Materials for

## Polymeric vanadyl species determine the low-temperature activity of V-based catalysts for the SCR of $NO_x$ with $NH_3$

Guangzhi He, Zhihua Lian, Yunbo Yu, Yang Yang, Kuo Liu, Xiaoyan Shi, Zidi Yan, Wenpo Shan, Hong He*

*Corresponding author. Email: honghe@rcees.ac.cn

Published 30 November 2018, *Sci. Adv.* **4**, eaau4637 (2018)
DOI: 10.1126/sciadv.aau4637

**This PDF file includes:**

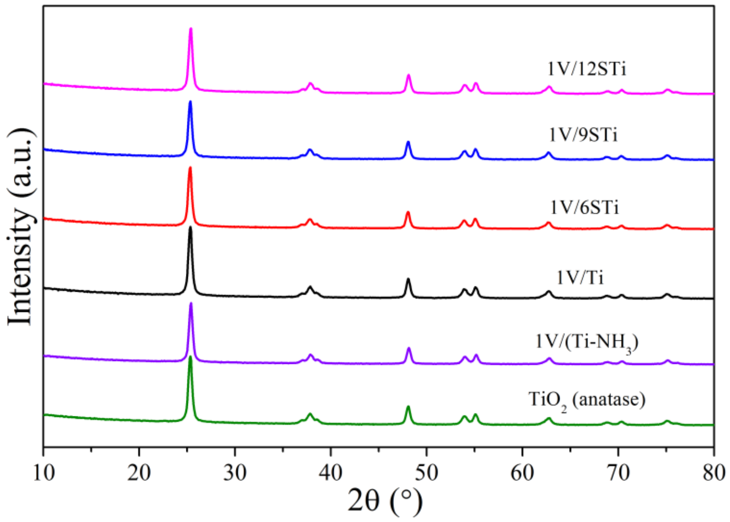

**Fig. S1. XRD patterns of vanadia/TiO$_2$ samples.**

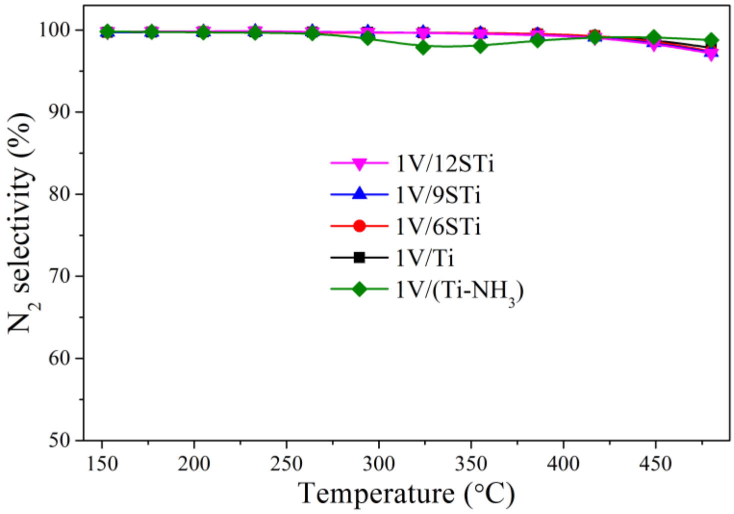

**Fig. S2. N$_2$ selectivity as a function of temperature in the feed gas of 500 ppm NO/500 ppm NH$_3$/5.0 vol % O$_2$/N$_2$ (200,000 hour$^{-1}$).**

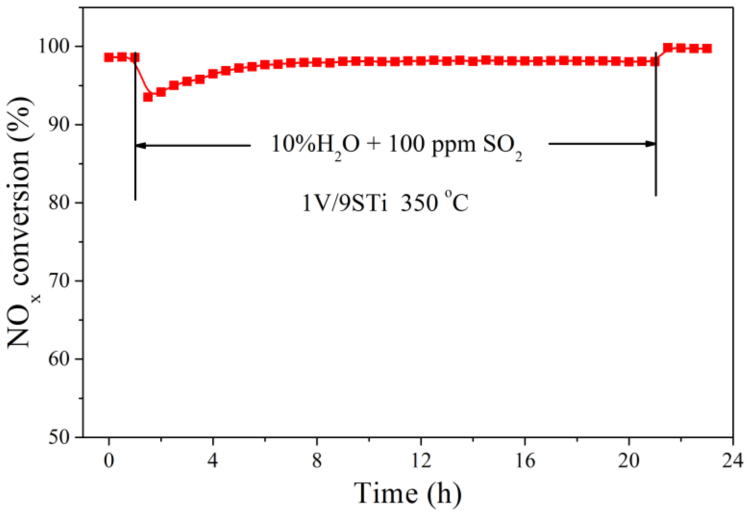

**Fig. S3. Effect of $H_2O$ and $SO_2$ on $NO_x$ conversion over the 1V/9STi catalyst at 350°C in the feed gas of 500 ppm NO/500 ppm $NH_3$/5.0 vol % $O_2/N_2$ (200,000 hour$^{-1}$).**

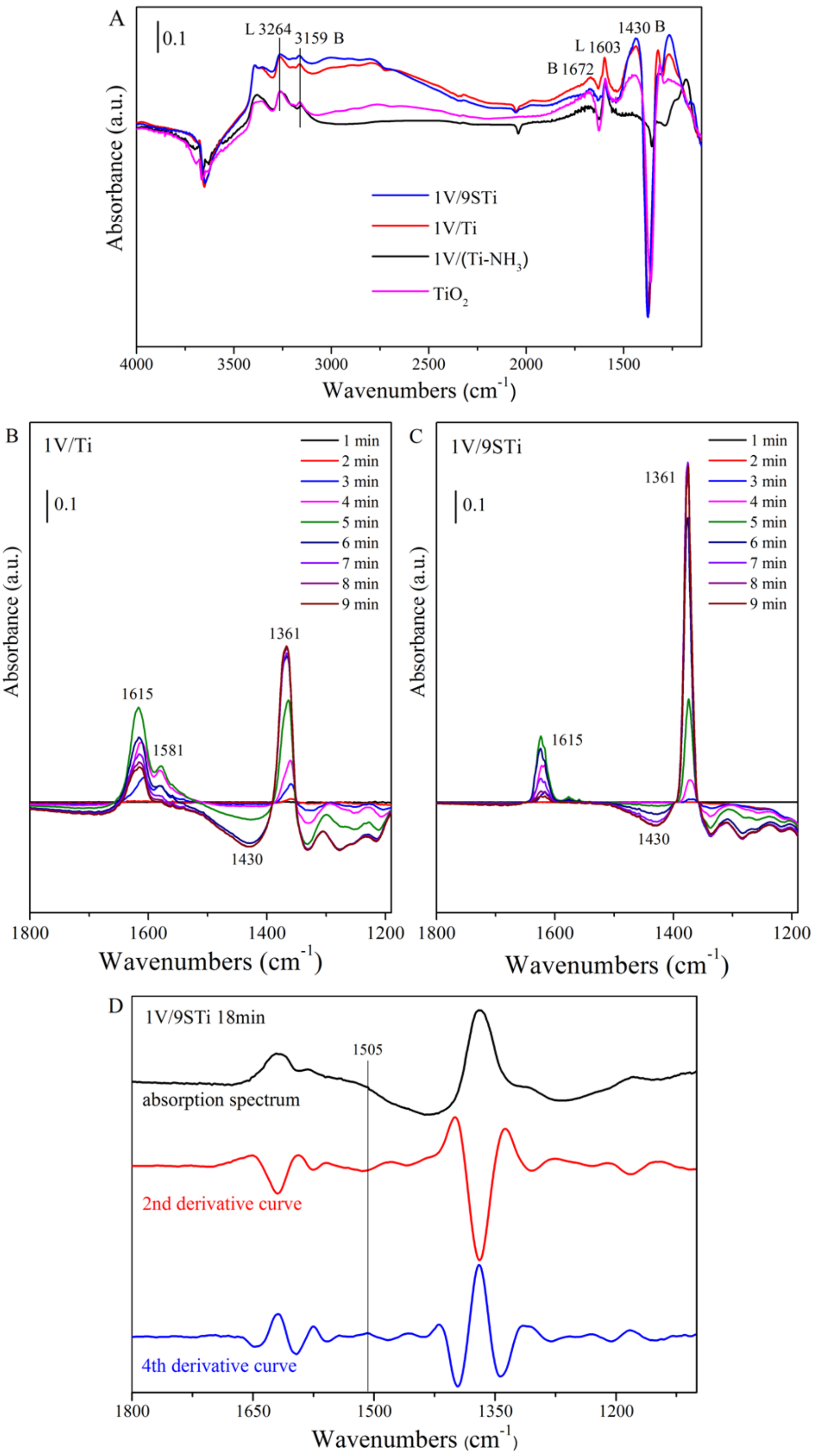

**Fig. S4. DRIFT spectra of $NH_3$ and NO + $O_2$ adsorption on the vanadia/$TiO_2$ catalysts.** (**A**) $NH_3$ adsorption on the vanadia/$TiO_2$ catalysts and $TiO_2$ support at 150°C. L: Lewis acid sites; B: Brønsted acid sites. (**B**) and (**C**) NO + $O_2$ adsorption on 1V/Ti and 1V/9STi catalysts pretreated with

$NH_3$ at 250 $^{o}$C and the $NH_3$ adsorption as the background. (**D**) $NH_3$-pretreated 1V/9STi sample after the flow of NO + $O_2$ for 18 min at 150$^{o}$C and the second and fourth derivative spectra.

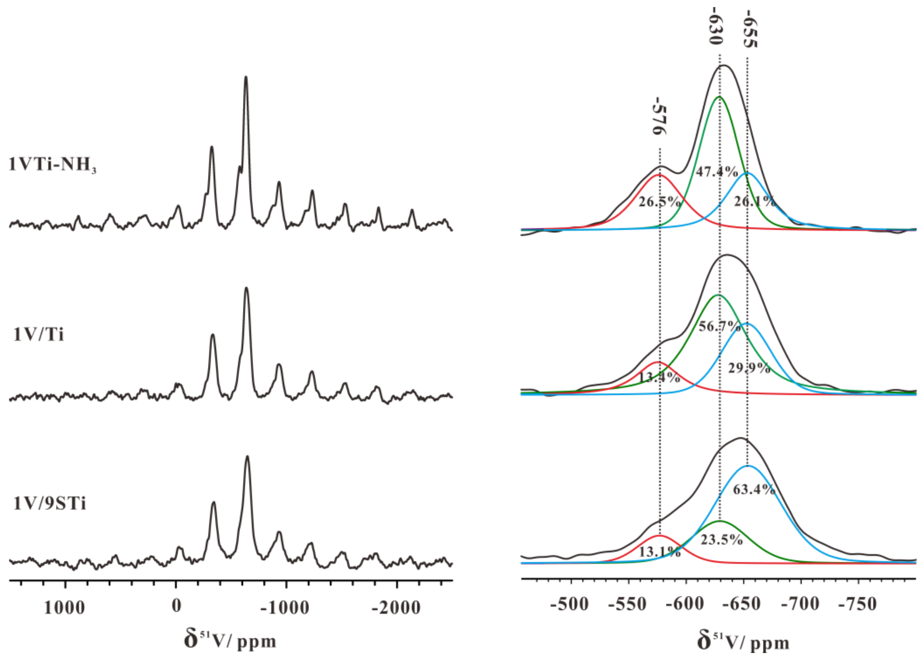

**Fig. S5. NMR spectra of vanadia/$TiO_2$ samples.** Decompositions of the $^{51}$V central-band NMR spectra are shown on the right. The chemical shift of the peak center and the percentage of the peak area normalized to the total peak area of the central-band spectra are presented at the top of each deconvoluted peak.

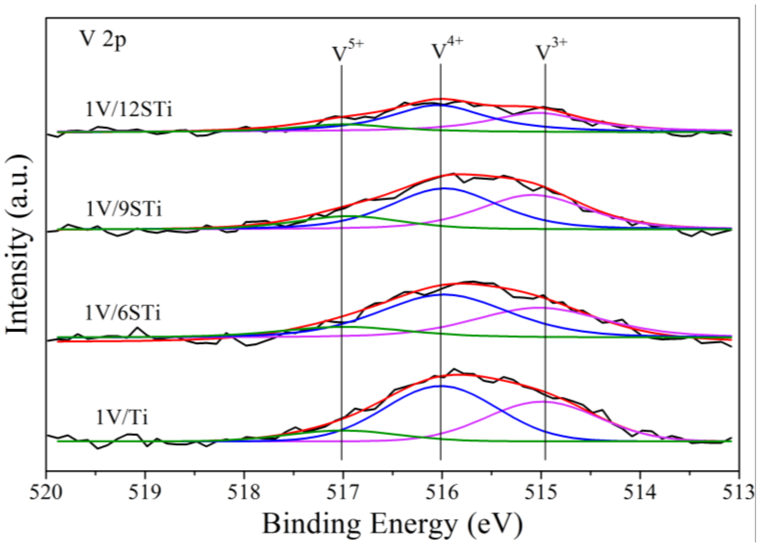

**Fig. S6. V 2p XPS spectra of vanadia/$TiO_2$ samples.**

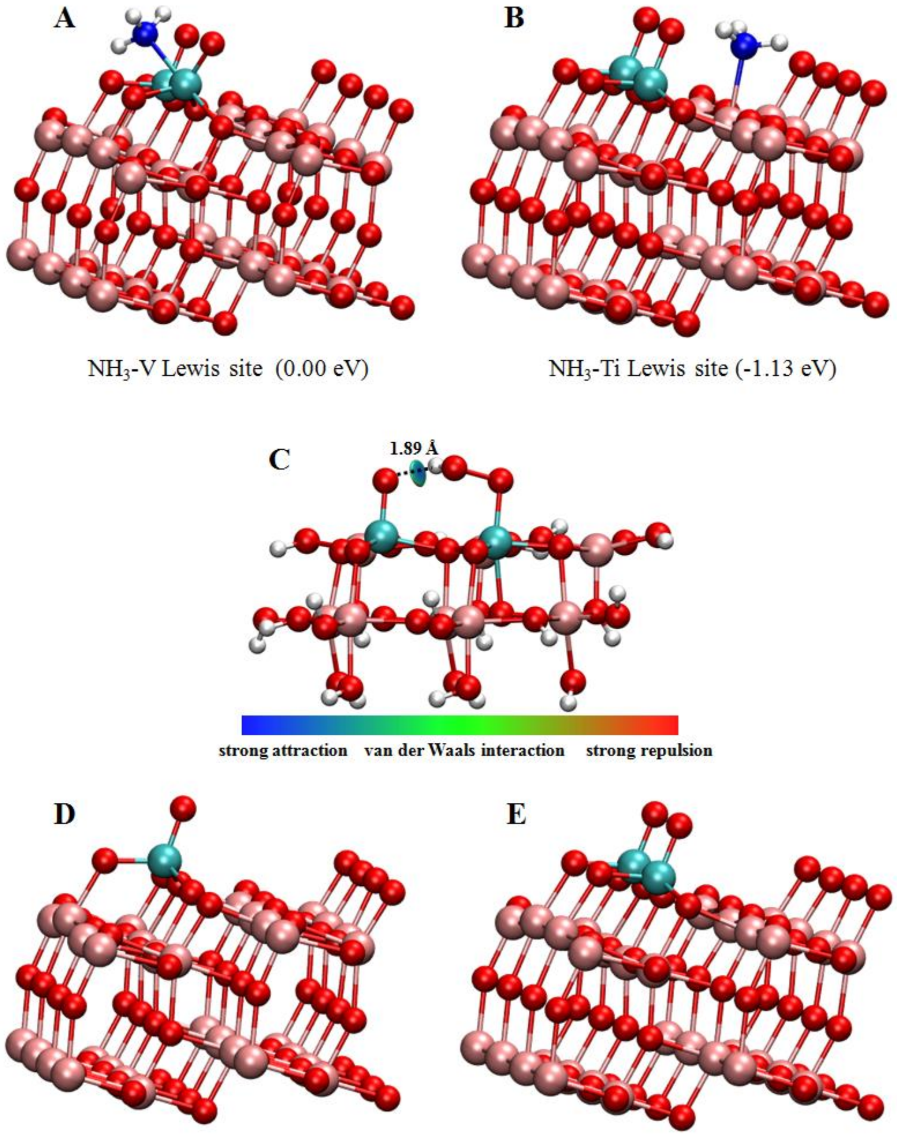

$NH_3$-V Lewis site (0.00 eV)

$NH_3$-Ti Lewis site (-1.13 eV)

**Fig. S7. Models used in DFT calculations.** (**A**) and (**B**) Relative energies and geometries of $NH_3$ adsorbed at the V and Ti sites on vanadia/$TiO_2$ surfaces. (**C**) The VOOH intermediate on dimeric vanadia/$TiO_2$ surfaces and reduced density gradient (RDG) isosurfaces colored by the values of sign[$\lambda_2$(r)]$\rho$(r). (**D**) and (**E**) Monomeric and dimeric vanadia/$TiO_2$ models used to calculate the catalytic reaction pathways. Red, pink, cyan, blue, and white circles denote O, Ti, V, N, and H atoms, respectively.

$\lambda_2$ is the second largest eigenvalue of a Hessian matrix of the electron density. The color bar shows the blue-green-red scale ranging from -0.04 to 0.02 a.u. Blue, green, and red represent the strong attraction (e.g., hydrogen bonding), van der Waals interaction, and strong repulsion (e.g., steric repulsion), respectively. The reduced density gradient of the electron density [RDG(r)], defined as $|\nabla \rho(r)/\rho^{4/3}(r)|$ (*39*), were analyzed using a wavefunction (WFN) file with the Multiwfn package (*40*). The standard wavefunction (WFN) file was produced by a DFT calculation performed at the B3LYP/6-31G(d) level with the Gaussian 09 package (*41*). The cluster model was constructed based on the VASP-optimized geometries. The dangling bonds of the boundary O atoms were saturated with H atoms. During the DFT calculation, the dimeric vanadia/$TiO_2$ model was fixed at the VASP-optimized positions and all remaining H atoms were allowed to relax.

There is a significant blue region between the VOOH group and the adjacent V=O group, clearly indicating the formation of a hydrogen bond. The strong H-bond interaction enhances the stability of the VOOH intermediate on dimeric vanadia/$TiO_2$ surfaces, and allows it to maintain a relatively long lifetime.

**Table S1. Relative surface atomic concentrations of vanadia/$TiO_2$ samples obtained from XPS.**

| Catalysts | V atomic % | S atomic % | Ti atomic % | O atomic % |
|---|---|---|---|---|
| Ti-$NH_3$ | -- | 0 | 30.42 | 69.58 |
| 1V/(Ti-$NH_3$) | 0.78 | 0.46 | 26.66 | 72.10 |
| 1V/Ti | 0.65 | 1.83 | 26.65 | 70.87 |
| 1V/6STi | 0.58 | 2.34 | 26.96 | 70.12 |
| 1V/9STi | 0.46 | 3.06 | 21.37 | 75.11 |
| 1V/12STi | 0.49 | 4.30 | 21.35 | 73.86 |

**Table S2. $N_2$ physisorption results of vanadia/$TiO_2$ samples.**

| Catalysts | Specific surface area ($m^2$/g) | Pore diameter (nm) | Pore volume (cc/g) |
|---|---|---|---|
| 1V/(Ti-$NH_3$) | 90.45 | 14.97 | 0.34 |
| 1V/Ti | 83.06 | 20.04 | 0.42 |
| 1V/6STi | 79.05 | 19.19 | 0.38 |
| 1V/9STi | 79.11 | 18.62 | 0.37 |
| 1V/12STi | 74.60 | 18.40 | 0.34 |

**Table S3. A comparison of reaction rates and TOFs between our catalyst and reported commercial catalysts for the SCR of NO with $NH_3$ at 200°C.**

| Samples | $V_2O_5$ loading (%) | NO conversion (%) | Reaction rates (mol $g^{-1}$ $s^{-1}$) | TOF ($s^{-1}$) |
|---|---|---|---|---|
| 1V/9STi | 1 | 18.7 | $2.7\times10^{-7}$ | $2.4\times10^{-3}$ |
| 1V/Ti | 1 | 7.5 | $1.1\times10^{-7}$ | $9.7\times10^{-4}$ |
| $V_2O_5$-$WO_3$/$TiO_2$ (fresh sample) in Ref. 18 | 0.432 | 6.5 | $8.9\times10^{-8}$ | $1.9\times10^{-3}$ |
| $V_2O_5$-$WO_3$/$TiO_2$ in Ref. 19 | 1.68 | 30.0 | $2.0\times10^{-7}$ | $1.1\times10^{-3}$ |

The reaction rate (r) was calculated according to the following equation

$$r = \frac{n_{NO-reduced}}{m_{cat}t} = \frac{n_{NO}x}{m_{cat}t} \tag{1}$$

where $n_{NO\text{-reduced}}$, $m_{cat}$, t, x and $n_{NO}$ are the amount of NO reduced, the catalyst weight, time, NO conversion and the amount of NO introduced into the reactor, respectively.

$n_{NO}$ was calculated by the following equation

$$n_{NO} = \frac{p_{NO}V}{RT} = \frac{py_{NO}V}{RT} \tag{2}$$

where p, $p_{NO}$, $y_{NO}$, V, R, and T are the atmospheric pressure, the NO pressure, concentration of NO, volume, gas constant, and temperature, respectively.

Therefore, r was calculated based on the equation

$$r = \frac{n_{NO-reduced}}{m_{cat}t} = \frac{n_{NO}x}{m_{cat}t} = \frac{py_{NO}Vx}{m_{cat}tRT} = \frac{py_{NO}x}{m_{cat}RT}\frac{V}{t} \tag{3}$$

Then, TOF was calculated according to the following equation

$$TOF = \frac{r}{n_V} \tag{4}$$

where $n_V$ is the number of vanadium in 1 g catalyst.

**Table S4. Vanadium valence distribution in vanadia/$TiO_2$ samples obtained from XPS.**

| | $V^{3+}$/V (%) | $V^{4+}$/V (%) | $V^{5+}$/V (%) |
|---|---|---|---|
| 1V/Ti | 37.5 | 52.3 | 10.2 |
| 1V/6ST | 35.6 | 51.7 | 12.7 |
| 1V/9ST | 38.8 | 46.3 | 14.9 |
| 1V/12ST | 34.6 | 50.7 | 14.7 |

**Table S5. $NH_3$-SCR de-$NO_x$ reaction rate constants (*k*) at 493.15 K (220°C) over the monomeric and dimeric vanadia/$TiO_2$ surfaces.**

| Surface vanadyl species | Rate constants ($k$, $s^{-1}$) |
|---|---|
| Monomeric vanadia | $1.4\times10^{-3}$ |
| Dimeric vanadia | $2.1\times10^{-1}$ |

The reaction rate constants ($k$) were calculated based on the transition state theory formula including the Wigner tunneling correction (Eq. 5), where $\chi$ is the Wigner transmission coefficient (Eq. 6), $k_b$ is the Boltzmann constant, $h$ is the Planck constant, $T$ is the temperature, Im($\nu^{\neq}$) is the imaginary frequency, and $\Delta E$ is the difference in energies between the transition state and the reactant complex in the rate-determining step

$$k = \chi \frac{k_b T}{h} \exp(-\frac{\Delta E}{k_b T}) \tag{5}$$

$$\chi = 1 + \frac{1}{24}(\frac{h\,\mathrm{Im}(\nu^{\neq})}{k_b T})^2 \tag{6}$$

**Table S6. DFT-calculated structural parameters and energy barriers (Δ*E*) for the formation of the first $NH_2NO$ intermediate over the monomeric vanadia/$TiO_2$ surfaces (i.e., the A→C process in Figs. 2A and 3) with different computational settings.**

| | N-N distances (Å) | | | Δ*E* (eV) |
|---|---|---|---|---|
| | A* | B | C | |
| Manuscript | 3.886 | 2.487 | 1.298 | 1.358 |
| 2×1×1 mesh of *k*-points | 3.887 | 2.487 | 1.298 | 1.358 |
| cutoff 600 eV | 3.887 | 2.489 | 1.297 | 1.360 |

*The A, B, and C letters correspond to the structures shown in Fig. 3.